Thermochimica Acta, 142 (1989) 89–105
Elsevier Science Publishers B.V., Amsterdam – Printed in The Netherlands

THERMAL INVESTIGATION AND STEREOCHEMICAL STUDIES OF SOME CYCLIC DIAMINE COMPLEXES OF NICKEL(II), ZINC(II) AND CADMIUM(II) IN THE SOLID STATE. PART III

LANGONJAM KANHAI SINGH and SAMIRAN MITRA *

Department of Chemistry, Manipur University, Canchipur Imphal-795 003 (India)

(Received 31 May 1988)

ABSTRACT

Monochloroacetato (MCA) cyclic diamine (piperazine (pipz); *N*-methylpiperazine (mpipz); 1,4-diazacycloheptane (dach)) complexes of nickel(II), zinc(II) and cadmium(II) were synthesized. A thermal investigation was carried out and the stereochemical changes which occurred during thermal decomposition were studied. The complexes were characterized with the help of elemental and thermal analyses and IR spectral and magnetic moment data. They were found to have the compositions: $[Ni(pipz)(MCA)_2(H_2O)_2]$, $[NiL_2(MCA)_2]\cdot 2H_2O$ (L = mpipz or dach), $[Zn(pipz)(MCA)_2]\cdot H_2O$, $[Zn(mpipz)(MCA)_2]\cdot 2H_2O$, $[Zn(dach)(MCA)_2]$, $[Cd(pipz)_2(MCA)_2]\cdot 2H_2O$ and $[CdL_2(MCA)_2]$ (L = mpipz or dach). Attempts to prepare *N*,*N*′-dimethylpiperazine complexes failed. Configurational and conformational changes were studied using thermal analysis and IR spectral and magnetic moment (in the case of nickel(II) complexes) data. All the complexes of nickel(II) and cadmium(II) appeared to possess an octahedral structure, whereas those of zinc(II) appeared to be tetrahedral. Thermodynamic parameters such as activation energy $E_a^\star$, enthalpy change ΔH and entropy change ΔS for the dehydration and decomposition reactions of the complexes were evaluated using some standard methods. The order of stability of the complexes (with respect to $E_a^\star$) follows the trend pipz > mpipz > dach. A linear correlation obtained by plotting $E_a^\star$ vs. ΔS shows that a system with a higher entropy change ΔS will require less energy $E_a^\star$ for decomposition.

INTRODUCTION

As a continuation of our earlier studies [1–3], this work reports the thermal investigation and stereochemical studies of monochloroacetato cyclic diamine complexes of Ni^{II}, Zn^{II} and Cd^{II} in the solid state. On heating under non-isothermal conditions, the complexes first undergo dehydration (in some cases) followed by decomposition in a single or multiple step(s) (see later, Table 3). In these complexes, before pyrolysis, the cyclic diamines function as bidentate chelating agents (boat form) as indicated by the larger

* To whom correspondence should be addressed.

0040-6031/89/$03.50

number of IR bands in the 700–1400 cm^{-1} region than that of the free cyclic ligand which exists in the chair form [1–4]. The monochloroacetate ion may function as a unidentate ligand in many cases and as a bridging bidentate ligand in a few cases as shown by the IR spectral data [3,5] (see later, Table 2). In general, the frequency of the asymmetric vibration of CO_2^- of MCA ($\nu_{as}(CO_2^-)$) increases, while the frequency of the symmetric vibration is the same or decreases as compared with the frequency of CO_2^- of the acetate ion [3,5]. This is in agreement with earlier findings [5–7]. On heating under non-isothermal conditions, all the complexes undergo decomposition via some intermediate complexes. The cyclic diamines in these intermediates function as bridging bidentate ligands (chair form) [3,4] and as both chelating and bridging agents in some Cd^{II} complexes. The monochloroacetate ion acts as a unidentate agent, a bridging bidentate agent or a bidentate agent. From these considerations, the stereochemical changes of the complexes and intermediates (heated products) are presented in Scheme 1. Some thermodynamic parameters such as E_a^*, ΔH and ΔS for the dehydration and decomposition reactions of the complexes in the solid state are evaluated. Some useful conclusions (as in refs. 1–3) are drawn and the electron-withdrawing effect of chlorine on the CO_2^- of $CH_2ClCO_2^-$ (MCA) is reported. Furthermore, the effects of *N*-alkylation and increasing ring size of the cyclic ligand on the stability of the complexes is discussed.

EXPERIMENTAL

Materials and methods

Metal carbonates of AnalaR grade were used as received. Metal monochloroacetates were freshly prepared by neutralizing monochloroacetic acid with an excess of the metal carbonate, followed by slow evaporation of the monochloroacetate solution obtained by filtration. Piperazine (Merck, F.R.G.), *N*-methylpiperazine, *N,N'*-dimethylpiperazine and 1,4-diazacycloheptane (homopiperazine) (Fluka AG, Switzerland) were used as received. Diethyl ether and ethanol were dried by standard procedures [1]. Acetone (AnalaR) obtained from BDH was used as received.

Preparation of complexes

[Ni(pipz)(MCA)$_2$(H$_2$O)$_2$]

A clear solution of freshly prepared nickel monochloroacetate (~ 0.900 g; 3 mmol) in dry ethanol (50 cm^3) was treated with the ligand (~ 0.516 g; 6 mmol) in dry ethanol (20 cm^3) with constant stirring. A bluish green precipitate of the nickel complex was obtained. This coalesced when treated with a little dry ether. The complex was collected by filtration under suction,

Scheme 1

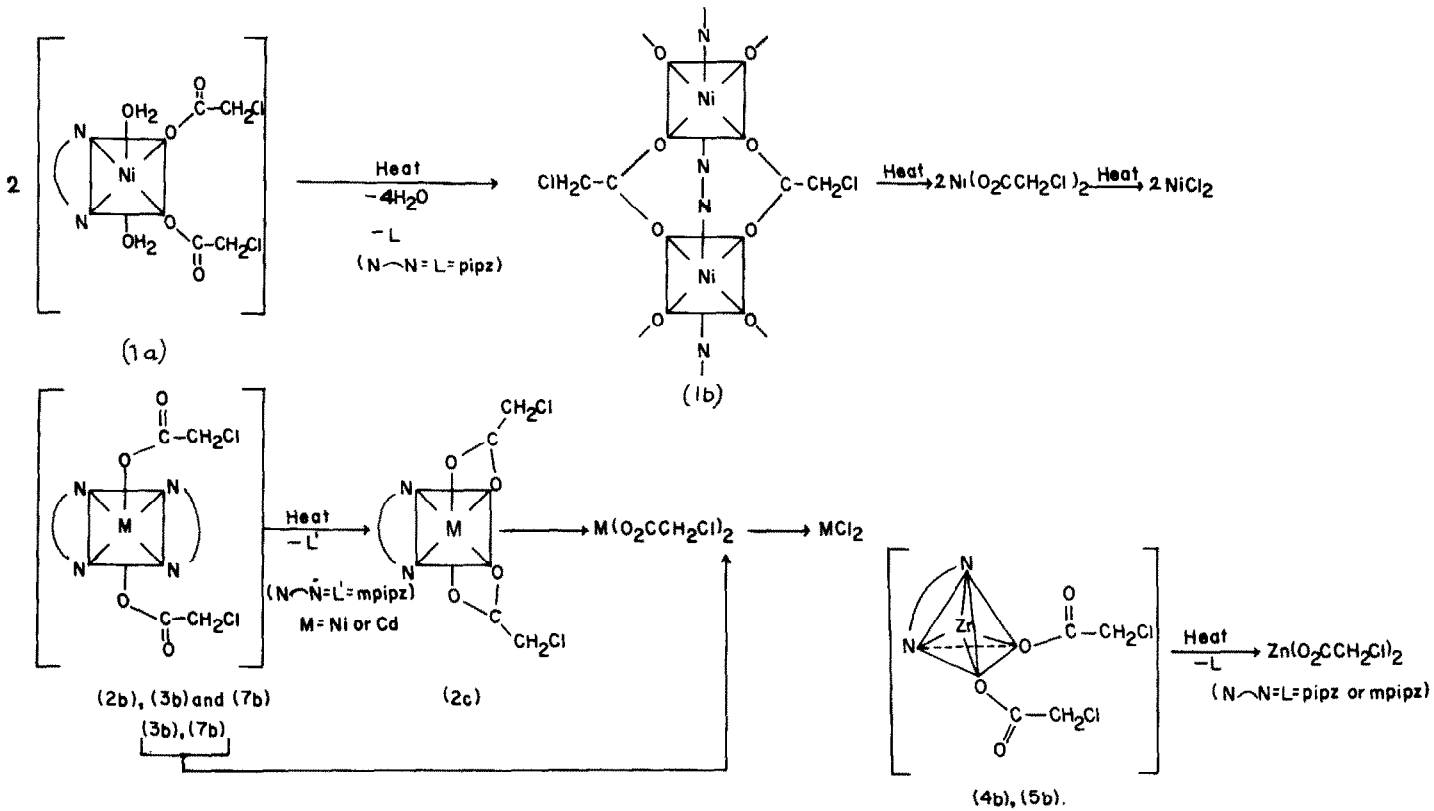
2
Heat
$-4H_2O$
$-L$
(N⌒N = L = pipz)
(1a)
(1b)
Heat
$2\,Ni(O_2CCH_2Cl)_2$
Heat
$2\,NiCl_2$
Heat
$-L'$
(N⌒N=L'=mpipz)
M = Ni or Cd
(2b), (3b) and (7b)
(3b), (7b)
(2c)
$M(O_2CCH_2Cl)_2$
MCl_2
Heat
$-L$
$Zn(O_2CCH_2Cl)_2$
(N⌒N=L=pipz or mpipz)
(4b), (5b).

Scheme 1 (continued)

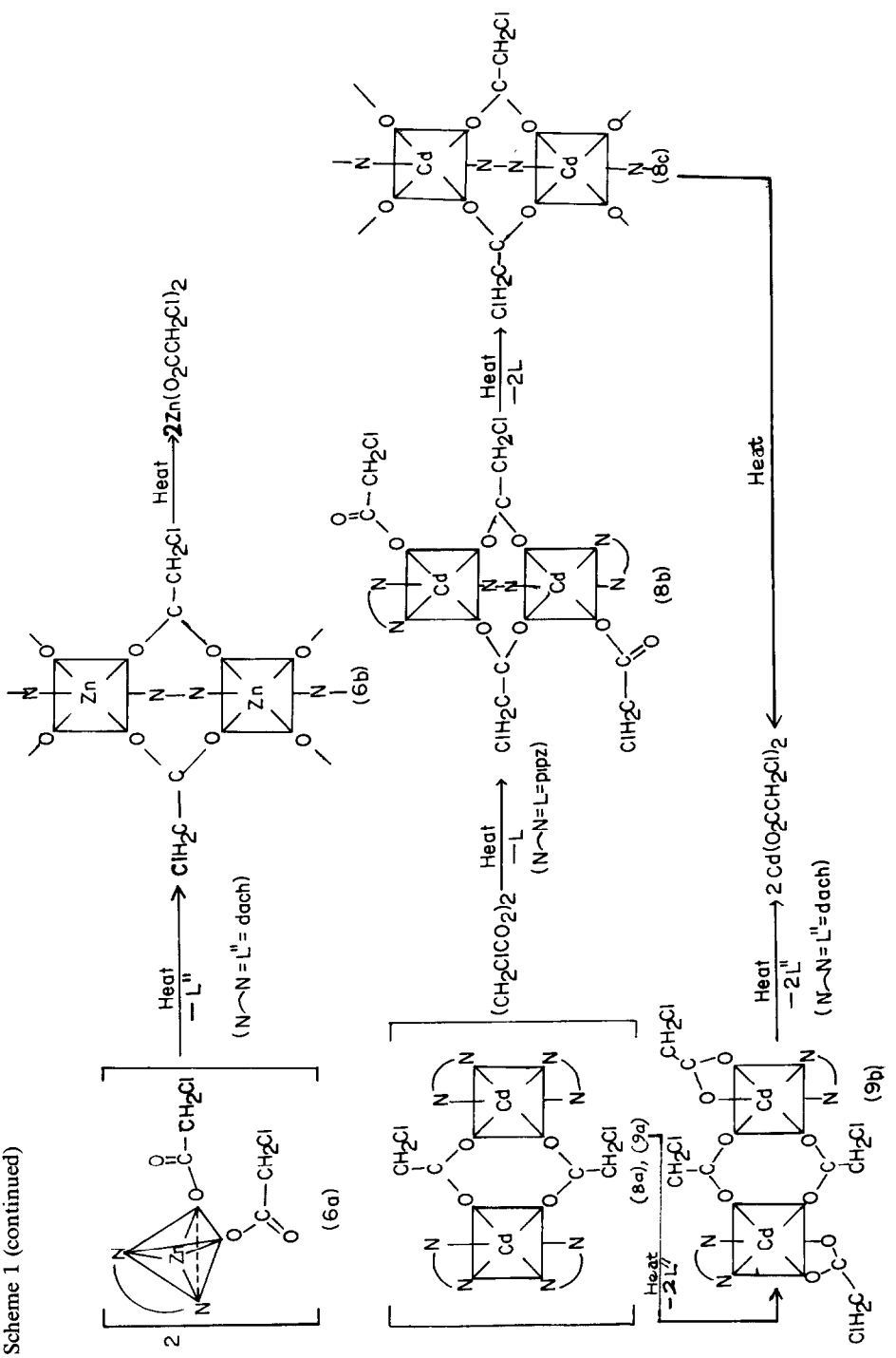

washed with dry ethanol (3–4 times), followed by a little dry diethyl ether (2–3 times), and was kept over fused calcium chloride in a desiccator. Yield: 0.860 g, ~ 70%.

$[Ni(mpipz)_2(MCA)_2] \cdot 2H_2O$

A solution of freshly prepared nickel monochloroacetate (~ 3 mmol) in 50 cm^3 of dry ethanol was treated with the ligand (mpipz) (~ 0.7 cm^3 of density 0.903 g cm^{-3}; 6 mmol) with constant stirring. Excess dry diethyl ether was added and a bluish green, oily complex was obtained. The oily complex (collected after decanting the supernatant liquid) was treated with acetone with vigorous stirring until the complex crystallized. The complex was collected by filtration, washed with a little acetone and dried over fused calcium chloride in a desiccator. Yield: ~ 50%.

$[Ni(dach)_2(MCA)_2] \cdot 2H_2O$

The ligand (dach) (~ 0.600 g; 6 mmol) in dry ethanol (20 cm^3) was added to a dry ethanolic solution (50 cm^3) of the freshly prepared nickel monochloroacetate (~ 3 mmol). Excess dry diethyl ether was added and a yellowish green precipitate of the complex appeared. The complex was collected by filtration, washed with acetone and dried over fused calcium chloride in a desiccator. Yield: ~ 70%.

$[ZnL(MCA)_2] \cdot xH_2O$ (L = pipz, mpipz or dach, x = 1 for pipz, 2 for mpipz and 0 for dach)

The ligand (~ 6 mmol) in dry ethanol (20 cm^3) was treated with a solution (50 cm^3) of the freshly prepared zinc monochloroacetate (~ 0.860 g; 3 mmol) in dry ethanol. A white precipitate of the zinc complex was obtained. This was collected by filtration, washed with dry diethyl ether and kept over fused calcium chloride in a desiccator. Yield: ~ 50%–60%.

$[Cd(pipz)_2(MCA)_2] \cdot 2H_2O$ and $[CdL_2(MCA)_2]$(L = mpipz or dach)

These were prepared in the same way as the zinc complexes. Yield: ~ 60%–70%.

Elemental analysis, thermal investigation, IR spectroscopy and magnetic moment measurements

Nickel, zinc and cadmium were gravimetrically estimated by standard procedures [8]. Carbon, hydrogen and nitrogen were measured using Perkin–Elmer 240C and Carlo Erba 1106 elemental analysers. The results of the elemental analyses are given in Table 1. Thermal investigations (TG and DTA) were carried out using a Shimadzu DT-30 thermal analyser in

TABLE 1

Analytical (calculated values in parentheses) and magnetic data of monochloroacetato cyclic diamine [a] complexes of Ni^{II}, Zn^{II} and Cd^{II}

Complex	Colour	Analysis (%)				μ_{eff} (BM)
		M	C	H	N	
1a $[NiL(MCA)_2(H_2O)_2]$	Bluish green	15.80 (15.96)	26.59 (26.11)	4.45 (4.90)	7.80 (7.61)	3.31
2a $[NiL'_2(MCA)_2]\cdot 2H_2O$	Bluish green	12.02 (12.19)	34.78 (34.88)	6.50 (6.64)	11.53 (11.63)	3.16
3a $[NiL''_2(MCA)_2]\cdot 2H_2O$	Greenish yellow	11.84 (12.19)	34.69 (34.88)	6.54 (6.64)	12.24 (11.63)	3.25
4a $[ZnL(MCA)_2]\cdot H_2O$	White	18.85 (19.33)	27.93 (28.37)	4.45 (4.73)	8.37 (8.27)	
5a $[ZnL'(MCA)_2]\cdot 2H_2O$	White	17.10 (16.84)	27.95 (27.81)	5.33 (5.15)	6.94 (7.21)	
6a $[ZnL''(MCA)_2]$	White	17.93 (18.56)	29.98 (30.64)	4.61 (4.54)	7.35 (7.95)	
7a $[CdL_2(MCA)_2]\cdot 2H_2O$	White	21.80 (22.15)	28.88 (28.38)	5.83 (5.52)	11.44 (11.04)	
8a $[CdL'_2(MCA)_2]$	White	21.94 (22.51)	33.78 (33.64)	5.54 (5.61)	11.70 (11.21)	
9a $[CdL''_2(MCA)_2]$	White	21.89 (22.51)	33.31 (33.64)	5.22 (5.61)	11.59 (11.21)	

[a] L = piperazine (pipz), L' = *N*-methylpiperazine (mpipz) and L'' = 1,4-diazacycloheptane (dach).

dynamic nitrogen at a heating rate of 10 °C min^{-1}. α-Alumina was used as a standard. The activation energy E_a^* was evaluated from the TG curve using the equation of Horowitz and Metzger [9] and from the DTA curve using that of Borchardt and Daniels [10]. The enthalpy change ΔH was evaluated from the DTA curve using the relation $\Delta H = KA$, where K is the heat transfer coefficient (calibration or cell constant; the cell used was a platinum crucible and its constant K was evaluated from the data obtained using indium metal as a calibrant) and A is the total area under the particular DTA peak measured using a compensating planimeter with an optical tracer of Fuji Corona 027. The entropy change ΔS was calculated using the relation [11] $\Delta S = \Delta H/T_m$, where T_m is the DTA peak temperature in kelvin. IR spectra were recorded using Beckmann IR 20A and Perkin–Elmer 783 IR spectrometers. The KBr disc method was employed. The effective magnetic moments were evaluated from the values of gram susceptibilities measured with an EG and G PAR 155 vibrating sample magnetometer at room temperature. The solid residues obtained from pyrolysis were identified by qualitative analysis. Conductivity measurements could not be performed because the complexes were insoluble in most organic solvents.

RESULTS AND DISCUSSION

[Ni(pipz)(MCA)$_2$(H$_2$O)$_2$] (1a)

This complex has not been reported previously. It has a bluish green colour and the presence of water molecules is confirmed by the appearance of IR bands at 3400 cm^{-1} (ν(OH)) and 1600 and 1560 cm^{-1} (δ(HOH)) (Table 2). Furthermore, the weight loss in the TG curve of **1a** in the range 40–292 °C and the endothermic peak in the DTA curve at 85 °C (Fig. 1) correspond to two molecules of water. On pyrolysis, the complex **1a** first undergoes dehydration, followed by the loss of one-half of the cyclic ligand to form the complex [Ni(pipz)$_{0.5}$(MCA)$_2$] (**1b**) (Table 3). The complex **1b** is converted into $NiCl_2$ via the formation of Ni(MCA)$_2$. This takes place in two steps, 1(b) and 1(c), in the ranges 292–326 °C and 326–530 °C respectively (Fig. 1 and Table 3). Values of $E_a^{\star}$, ΔH and ΔS for the conversions **1a** → **1b**, **1b** → **1c** and **1c** → $NiCl_2$ are given in Table 3.

The bluish colour and the value of the effective magnetic moment (μ_{eff} = 3.31 BM) of **1a** suggest an octahedral structure. In this complex, the cyclic ligand (pipz) functions as a bidentate chelating agent in the boat form as shown by the greater number of IR spectral bands in the 700–1400 cm^{-1} region (Table 2) compared with the free ligand, which exists in the chair form [1–4]. The monochloroacetate ion (MCA; CH_2ClCOO^-) probably acts as a unidentate ligand. The unidentate nature is indicated by the values of the separation between the asymmetric and symmetric frequencies of MCA

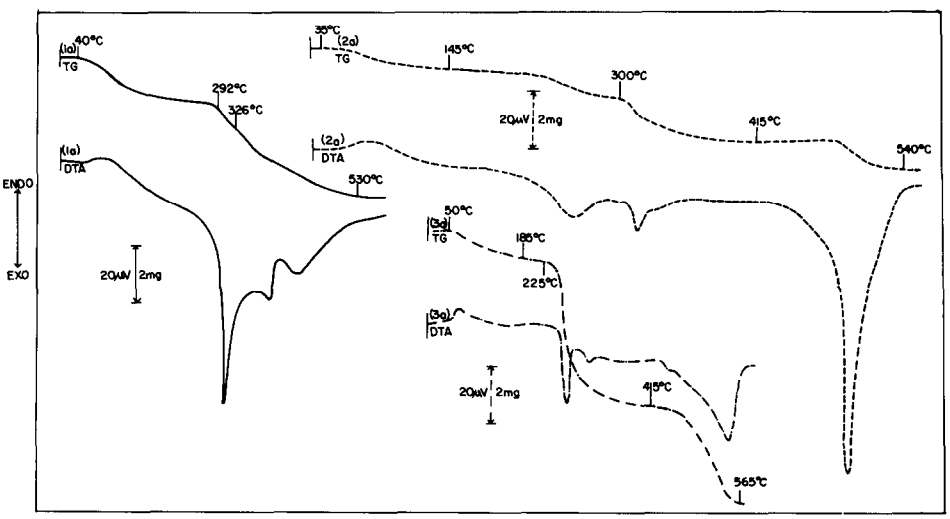

Fig. 1. Thermal curves of [Ni(pipz)(MCA)$_2$(H$_2$O)$_2$] (**1a**) (7.13 mg) (———), [Ni(mpipz)$_2$(MCA)$_2$]·2H$_2$O (**2a**) (6.96 mg) (- - - - - -) and [Ni(dach)$_2$(MCA)$_2$]·2H$_2$O (**3a**) (13.53 mg) (· – · – ·).

TABLE 2

IR spectral data (cm^{-1}) for monochloroacetato (MCA) cyclic diamine (L = pipz, L′ = mpipz and L″ = dach) complexes of Ni^{II}, Zn^{II} and Cd^{II}

Complex	ν(NH) + ν(OH)	$\nu(CH_2)$	δ(NH) + δ(HOH) + $\nu_{as}(CO_2^-)$	$\delta(CH_2)$ + $\nu_s(CO_2^-)$	$\Delta\nu$	$\rho_\omega(CH_2)$	τ(NH) + ρ_ω(NH) + $\tau(CH_2)$	Stretching vibrations of skeleton ν(C–N) + ν(C–C)	$\rho_r(CH_2)$	$\delta(CO_2^-)$ + ν(C–Cl)	ρ_r(NH) [b] + $\rho_r(CH_2)$ + ν(M–N)	ν(M–O)
1a $[NiL(MCA)_2(H_2O)_2]$	3400(vsbr)	2980(sh)	1600 (vsbr)	1455(sh)	190	1375(sh)	1340(sh)	1100(m)	940(vw)	810(m)	685(vw)	440(mbr) [a]
		2840(vw)	1560(sh)	1430(sh)	(215)		1330(m)	1050(vw)	900(sh)	735(ms) [a]	610(mbr)	280(m)
			1540(sh)	1410 (s)			1320(sh)	1025(vw)	850(m)			
			1510(w)	1385 (s)			1280(vw)	1010(vw)				
							1190(vw)	990(vw)				
							1160(vw)					
2a $[NiL'_2(MCA)_2]\cdot 2H_2O$	3300(vsbr)	3020(vw)	1660 (s)	1445 (s)	215	1380(w)	1335(sh)	1090(vw)	950(m)	840(w)	675(vw)	485(w)
		2980(vw)	1590 (vsbr)	1425(sh)	(250)	1345(sh)	1330(ms)	1080(vw)	920(w)	790(vw)	670(vw)	455(w)
		2940(w)		1410 (s)			1310(vw)	1070(vw)	910(w)	850(mbr)	590(vw)	430(w)
		2900(sh)					1300(w)	1050(vw)	860(m)		525(sh)	400(w)
		2860(w)					1290(w)	1035(w)			520(w)	370(m)
		2800(sh)					1260(w)	1025(w)				350(sh)
							1210(w)	1010(m)				310(vw)
							1200(sh)	990(m)				295(sh)
							1185(w)					290(w)
							1180(sh)					
							1150(ms)					
							1125(m)					
							1115(sh)					

3a $[NiL''_2(MCA)_2]\cdot 2H_2O$	3540(s)	3000(w)	1700(sh)	1495(sh)	240	1370(w)	1320(m)	1100(w)	940(w)	785(m)	700(w)	495(m)
	3430(s)	2980(vw)	1640 (vs)	1490(w)	(255)	1350(w)	1300(w)	1065(ms)	915(vw)	750(vw)	645(sh)	470(m)
	3290(s)	2960(sh)	1625(s)	1465(sh)			1285(vw)	1035(w)	885(m)		635(w)	420(w)
	3120(ms)	2940(m)	1580(sh)	1450(w)			1265(w)	995(w)	865(vw)		605(vw)	400(vw)
		2900(m)	1575(ms)	1430(w)			1250(vw)	985(m)	855(vw)		590(w)	365(vw)
		2880(m)	1500(w)	1400 (s)			1225(w)					325(vw)
				1385 (vs)			1150(m)					280(w)
							1130(vw)					
							1120(vw)					
4a $[ZnL(MCA)_2]\cdot H_2O$	3440(br)	2960(vw)	1645(sh)	1450(vw)	250	1355(sh)	1330(vw)	1090(w)	940(w)	810(sh)	700(s)	490(w)
	3200(w)	2880(vw)	1630 (vsbr)	1440(vw)			1250(m)	1050(vw)	895(sh)	790(vs)	670(w)	470(w)
	3180(sh)		1615(sh)	1410(m)			1150(w)	1025(w)	875(m)	740(w)	660(sh)	445(vw)
				1380 (s)			1125(w)	1000(w)			640(w)	420(vw)
											615(w)	400(w)
											600(sh)	325(w)
											575(w)	310(w)
											540(vw)	305(w)
											515(w)	280(m)
5a $[ZnL'(MCA)_2]\cdot 2H_2O$	3440(sbr)	2940(w)	1650(sh)	1480(vw)	210	1390(sh)	1330(m)	1100(wbr)	935(vw)	830(vw)	610(w)	470(wbr)
			1620 (vsbr)	1470(vw)		1370(sh)	1290(vw)	1020(vw)	910(w)	740(wbr)	595(vw)	390(wbr)
			1550(w)	1460(vw)		1345(sh)	1230(vw)	1005(vw)	890(w)		585(vw)	310(vw)
			1545(vw)	1440(vw)			1150(vw)				520(wbr)	290(w)
				1410 (s)								
6a $[ZnL''(MCA)_2]\cdot H_2O$	3560(sbr)	2970(w)	1650(sh)	1485(vw)	215	1380(sh)	1330(w)	1100(w)	930(vw)	780(w)	690(w)	470(wbr)
		2940(w)	1600 (vsbr)	1470(sh)		1375(sh)	1305(vw)	1065(w)	875(vw)	730(sh)	630(wbr)	390(vw)
		2900(w)	1560(w)	1450(w)		1360(sh)	1285(vw)	1050(vw)	850(vw)	720(w)	510(wbr)	280(m)
			1550(sh)	1410(w)		1355(vw)	1265(vw)	1020(wbr)				
			1505(w)	1385 (s)		1350(vw)	1250(vw)					
							1220(vw)					
							1150(vw)					
							1120(vw)					

TABLE 2 (continued)

Complex	ν(NH) + ν(OH)	$\nu(CH_2)$	δ(NH) + δ(HOH) + $\nu_{as}(CO_2^-)$	$\delta(CH_2)$ + $\nu_s(CO_2^-)$	$\Delta\nu$	$\rho_\omega(CH_2)$	τ(NH) + ρ_ω(NH) + $\tau(CH_2)$	Stretching vibrations of skeleton ν(C–N) + ν(C–C)	$\rho_r(CH_2)$	$\delta(CO_2^-)$ + ν(C–Cl)	ρ_r(NH) [b] + $\rho_r(CH_2)$ + ν(M–N)	ν(M–O)
7a $[CdL_2(MCA)_2]\cdot 2H_2O$	3440(mbr) 3220(w)	2960(w) 2850(vw)	1750(vw) 1600 (vsbr) 1560(sh)	1450(sh) 1400 (s)	200	1365(sh)	1330(m) 1255(m) 1180(wbr) 1120(w)	1100(wbr) 1070(vw) 1055(vw) 1020(sh) 1005(w)	940(vw) 905(vw) 875(w) 850(sh)	810(vw) 780(w)	700(wbr) 670(vw) 600(vw) 590(vw) 515(wbr) 505(w)	480(s) 470(s) sp 440(sh) 410(sh) 400(sh) 390(sh) 380(vw) 350(w) 340(sh)
8a $[CdL'_2(MCA)_2]$	3340(sbr) 3210(s)	2950(m) 2920(m) 2900(sh) 2850(vw) 2830(m) 2800(vw)	1720(vw) 1670(vw) 1590 (sbr)	1490(vw) 1440(m) 1430 (vs) 1415(ms) 1400(sh)	160	1385(vw) 1365(w) 1350(m) 1340(vw)	1340(vw) 1310(sh) 1305(w) 1285(m) 1265(ms) 1190(sh) 1170(ms) 1165(s) 1125(vs)	1090(s) 980(vs) 950(sh)	950(sh) 920(vw) 890(w) 855(s)	820(vw) 765(m)	700(wbr) 650(vw) 620(w) 590(vw) 520(mbr)	480(w) 460(sh) 415(w) 410(sh) 370(m) 290(vw)
9a $[CdL''_2(MCA)_2]$	3400(mbr) 3230(sh) 3210(s)	2950(w) 2920(w) 2880(vw)	1690(vw) 1645(vw) 1600 (sbr) 1550(w) 1530(w)	1450 (s) 1440(sh) 1425(m)	150	1375(vw) 1355(vw)	1310(vw) 1250(w) 1230(vw) 1130(ms)	1110(ms) 1090(m) 1080(sh) 1030(w) 1005(vs) 980(sh) 975(ms)	940(vw) 920(vw) 900(vw) 860(sh) 850(vs)	830(sh) 760(wbr)	700(wbr) 670(vw) 600(w)	460(vw) 400(vw) 375(vw) 355(vw) 280(w)

v, very; s, strong; m, medium; br, broad; w, weak; sh, shoulder; sp, split. [a] Frequencies overlap with those of coordinated water molecule, 735 cm^{-1} ($\rho_r(H_2O)$), 610 cm^{-1} ($\rho_\omega(H_2O)$) and 440 cm^{-1} (ν(M–O) in M–OH_2). [b] Frequencies above 650 overlap with those of δ(bending)(CO_2^-) and ν(stretching)(C–Cl).

($\Delta\nu = 190(215)$ cm^{-1}) (Table 2). This value of $\Delta\nu$ is higher than that of the unidentate acetate ion [3]. An increased value of $\Delta\nu$ has already been reported [5–7]. From these results it can be concluded that water molecules probably coordinate with the central metal ion Ni^{II}. The presence of coordinated water [5] in **1a** is also shown by its IR frequencies (735 cm^{-1} ($\rho_r(H_2O)$), 610 cm^{-1} ($\rho_w(H_2O)$) and 440 cm^{-1} (ν(MO))) in M–OH_2, in addition to the characteristic stretching and bending (scissoring) frequencies of the free water molecule already mentioned. These low frequencies of water may overlap with those of other modes of vibration (Table 2). The probable path of decomposition of **1a** is shown in Scheme 1.

$[Ni(mpipz)_2(MCA)_2] \cdot 2H_2O$ (2a)

This bluish green complex has not been reported previously. The presence of lattice water in **2a** is shown by the appearance of IR bands at 3300 cm^{-1} (ν(OH)) and 1660 and 1590 cm^{-1} (δ(HOH)) (Table 2). Moreover, the weight loss in the TG curve of **2a** in the range 35–145 °C and the endothermic peak at 65 °C in the DTA curve (Fig. 1) correspond to two water molecules. On non-isothermal heating, the complex **2a** first undergoes dehydration, followed by the decomposition of the anhydrous complex $[Ni(mpipz)_2(MCA)_2]$ (**2b**) into $NiCl_2$ via the formation of intermediates $[Ni(mpipz)(MCA)_2]$ (**2c**) and $Ni(MCA)_2$. This takes place in three steps, 2(b), 2(c) and 2(d), given in Table 3. This table also shows the values of $E_a^{\star}$, ΔH and ΔS for the conversions: **2a** → **2b**, **2b** → **2c**, **2c** → $Ni(MCA)_2$ and $Ni(MCA)_2 \rightarrow NiCl_2$.

In complex **2a**, the cyclic ligand (mpipz) acts as a bidentate chelating agent whereas the monochloroacetate ion (MCA) acts as a unidentate ligand as shown by the IR spectral data ($\Delta\nu = 215(250)$ cm^{-1}) in Table 2. Furthermore, the value of μ_{eff} of **2a** is 3.16 BM. Based on these facts, it can be concluded that **2a** has an octahedral configuration. The probable path of decomposition of **2a** is given in Scheme 1.

$[Ni(dach)_2(MCA)_2] \cdot 2H_2O$ (3a)

This greenish yellow complex has not been reported previously. The presence of lattice water is shown in the same way as in complex **2a**. On heating, **3a** first undergoes dehydration in the range 50–185 °C (Table 3 and Fig. 1) to give $[Ni(dach)_2(MCA)_2]$ (**3b**), which is converted into $NiCl_2$ via the formation of $Ni(MCA)_2$. This takes place in the ranges given in Table 3. The values of $E_a^{\star}$, ΔH and ΔS for the dehydration and decomposition reactions are also given in Table 3.

In complex **3a**, the dach ligand acts as a bidentate chelating agent, whereas the monochloroacetate ion probably functions as a monodentate ligand as indicated by the IR spectral data ($\Delta\nu = 255$ cm^{-1}). Therefore **3a**

TABLE 3

Thermal parameters of monochloroacetato cyclic diamine (pipz (L), mpipz (L′) or dach (L″)) complexes of Ni^{II}, Zn^{II} and Cd^{II}

Decomposition reaction		Temperature range (°C)	DTA peak temp (°C)		E_a^* (kJ mol^{-1})		Enthalpy change ΔH (kJ mol^{-1})	Entropy change ΔS (J K^{-1} mol^{-1})
			Endo	Exo	TG	DTA		
1(a) $[NiL(MCA)_2(H_2O)_2]$	→ $[NiL_{0.5}(MCA)_2]$	40–292	85	–	21.99	33.29	81.77	228.41
1(b) $[NiL_{0.5}(MCA)_2]$	→ $Ni(MCA)_2$	292–326	–	300	205.58 (79.88)	61.58	255.87	446.54
1(c) $Ni(MCA)_2$	→ $NiCl_2$	326–530	–	375, 425	55.24	–	–	–
2(a) $[NiL'_2(MCA)_2]\cdot 2H_2O$	→ $[NiL'_2(MCA)_2]$	35–145	65	–	41.96	51.23	59.86	177.10
2(b) $[NiL'_2(MCA)_2]$	→ $[NiL'(MCA)_2]$	145–300	–	257	47.33 (54.97)	150.76	100.72	190.04
2(c) $[NiL'(MCA)_2]$	→ $Ni(MCA)_2$	300–415	–	312	145.06	141.59	51.27	87.64
2(d) $Ni(MCA)_2$	→ $NiCl_2$	415–540	–	493	256.23	215.71	874.59	1141.76
3(a) $[NiL''_2(MCA)_2]\cdot 2H_2O$	→ $[NiL''_2(MCA)_2]$	50–185	68	–	24.32	27.73	41.06	120.41
3(b) $[NiL''_2(MCA)_2]$	→ $Ni(MCA)_2$	225–415	–	270, [a] 308	116.21	92.19	51.28	94.44
3(c) $Ni(MCA)_2$	→ $NiCl_2$	415–565	–	440, 540	195.06	216.76	238.35	293.17
4(a) $[ZnL(MCA)_2]\cdot H_2O$	→ $[ZnL(MCA)_2]$	50–185	100	–	29.37	34.95	38.51	103.24
4(b) $[ZnL(MCA)_2]$	→ $Zn(MCA)_2$	200–365	–	325, 365	50.14	–	–	–

4(c) $Zn(MCA)_2$	→ ZnO	365–640	–	440, 600 [a]	56.50	–	337.03	386.06
5(a) $[ZnL'(MCA)_2]\cdot 2H_2O$	→ $[ZnL'(MCA)_2]$	30–150	90	–	29.85	37.52	46.27	127.47
5(b) $[ZnL'(MCA)_2]$	→ $Zn(MCA)_2$	150–365	219	345	29.96	–	–	–
6(a) $[ZnL''(MCA)_2]$	→ $[ZnL''_{0.5}(MCA)_2]$	40–288	–	155	14.33	56.49	47.04	109.91
6(b) $[ZnL''_{0.5}(MCA)_2]$	→ $Zn(MCA)_2$	288–360	–	345	157.13 (133.64)	123.55	112.98	182.82
6(c) $Zn(MCA)_2$	→ $ZnCl_2$	360–620	–	450, 550	55.28	–	–	–
7(a) $[CdL_2(MCA)_2]\cdot 2H_2O$	→ $[CdL_2(MCA)_2]\cdot H_2O$	35–109	100	–	39.17	41.94	71.05	190.48
7(b) $[CdL_2(MCA)_2]\cdot H_2O$	→ $[CdL_2(MCA)_2]$	109–188	188	–	48.86	49.24	54.33	119.93
7(c) $[CdL_2(MCA)_2]$	→ $Cd(MCA)_2$	188–335	–	310	87.48	110.38	71.05	121.87
7(d) $Cd(MCA)_2$	→ $CdCl_2$	335–520	–	446	78.89	97.01	291.05	404.80
8(a) $[CdL'_2(MCA)_2]$	→ $[CdL'_{1.5}(MCA)_2]$	80–115	–	106	81.01	91.01	113.42	299.26
8(b) $[CdL'_{1.5}(MCA)_2]$	→ $[CdL'_{0.5}(MCA)_2]$	140–178	–	170	191.82	174.23	65.02	146.77
8(c) $[CdL'_{0.5}(MCA)_2]$	→ $Cd(MCA)_2$	178–210	–	200	191.33	–	–	–
9(a) $[CdL''_2(MCA)_2]$	→ $[CdL''(MCA)_2]$	40–250	–	235	13.28	–	159.98	314.92
9(b) $[CdL''(MCA)_2]$	→ $Cd(MCA)_2$	250–370	–	280	83.38	–	77.80	140.69
9(c) $Cd(MCA)_2$	→ $CdCl_2$	370–565	–	535	71.93	283.15	343.67	425.33

[a] DTA peak temperature used for the calculation of entropy change. Values in parentheses were evaluated by the Coats and Redfern method [12].

possesses an octahedral structure. This is also supported by the value of the effective magnetic moment ($\mu_{eff} = 3.25$ BM). The probable path of decomposition of **3a** is shown in Scheme 1.

*[Zn(pipz)(MCA)$_2$] · H$_2$O (**4a**), [Zn(mpipz)(MCA)$_2$] · 2H$_2$O (**5a**) and [Zn(dach)(MCA)$_2$] (**6a**)*

These white complexes have not been reported previously. On pyrolysis, complexes **4a** and **5a** first undergo dehydration in the ranges given in Table 3 to give the anhydrous complexes [Zn(pipz)(MCA)$_2$] (**4b**) and [Zn(mpipz)(MCA)$_2$] (**5b**). Both of these decompose into Zn(MCA)$_2$ in the ranges 200–365 and 150–365 °C respectively (Fig. 2). The complex **6a** decomposes to form [Zn(dach)$_{0.5}$(MCA)$_2$] (**6b**) in the range 40–288 °C, and **6b** decomposes into Zn(MCA)$_2$ in the range 288–360 °C (Fig. 2). The weight loss in the thermal curve (TG) of **4a** shows that the final product is ZnO, whereas that of **6a** shows that the final product is ZnCl$_2$. These products are verified by qualitative analysis. Values of E_a^*, ΔH and ΔS for the dehydration and decomposition reactions of the complexes are given in Table 3.

The IR spectra of the complexes **4a**, **5a** and **6a** show that the cyclic ligands, which function as bidentate chelating agents, exist in the boat form [4] (Table 2). The MCA ions act as monodentate ligands [3,6,7,13]; the values of $\Delta\nu$ are 250 cm^{-1} for **4a**, 210 cm^{-1} for **5a** and 215 cm^{-1} for **6a**. Therefore these complexes possess a tetrahedral structure in which zinc has a coordination number of four; this is typical of zinc [14].

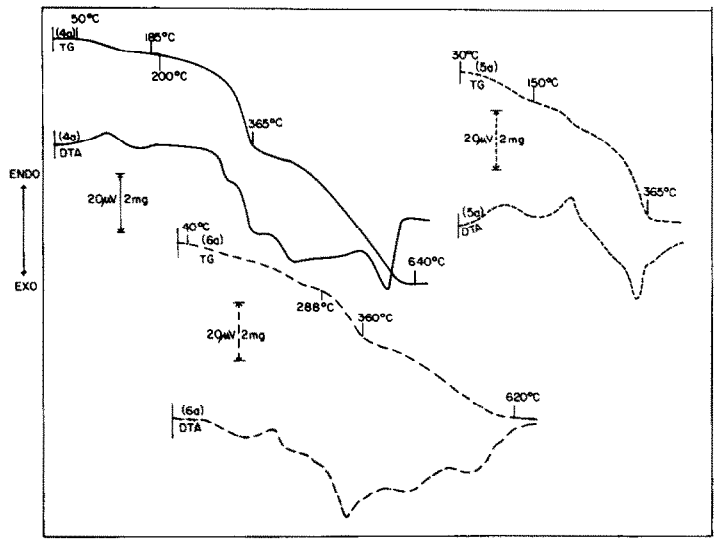

Fig. 2. Thermal curves of [Zn(pipz)(MCA)$_2$] · H$_2$O (**4a**) (11.40 mg) (———), [Zn(mpipz)(MCA)$_2$] · 2H$_2$O (**5a**) (13.31 mg) (- - - - -) and [Zn(dach)(MCA)$_2$] (**6a**) (10.80 mg) (· — · — ·).

The probable paths of decomposition of **4a**, **5a** and **6a** are given in Scheme 1.

$[Cd(pipz)_2(MCA)_2] \cdot 2H_2O$ (7a), $[Cd(mpipz)_2(MCA)_2]$ (8a) and $[Cd(dach)_2(MCA)_2]$ (9a)

These white complexes have not been reported previously. On pyrolysis, complex **7a** first undergoes dehydration to give the anhydrous complex $[Cd(pipz)_2(MCA)_2]$ (**7b**). This takes place in two steps in the ranges 35–109 and 109–188 °C respectively (Table 3 and Fig. 3). The complexes **7b**, **8a** and **9a** decompose to $Cd(MCA)_2$, $[Cd(mpipz)_{1.5}(MCA)_2]$ (**8b**) and [Cd(dach) $(MCA)_2$] (**9b**) in the ranges 188–335, 80–115 and 40–250 °C respectively (Fig. 3). Complex **8b** is converted into $Cd(MCA)_2$ via the formation of $[Cd(mpipz)_{0.5}(MCA)_2]$ (**8c**). Complex **9b** decomposes into $CdCl_2$ via the formation of $Cd(MCA)_2$. The ranges of conversion are given in Table 3, which also shows the values of the thermal parameters.

In all these complexes (**7a**, **8a** and **9a**) the cyclic ligands function as bidentate chelating agents. MCA probably functions as a unidentate ligand in **7a**; in **8a** and **9a**, MCA probably acts as a bridging bidentate agent as shown by the IR data [5,13,15,16]; $\Delta\nu$ is 200 cm^{-1} for **7a**, 160 cm^{-1} for **8a** and 150 cm^{-1} for **9a** (Table 2). As a result, **7a** possesses an octahedral structure and exists in a monomeric form, whereas **8a** and **9a** have octahedral structures and exist in dimeric forms. These are depicted in Scheme 1.

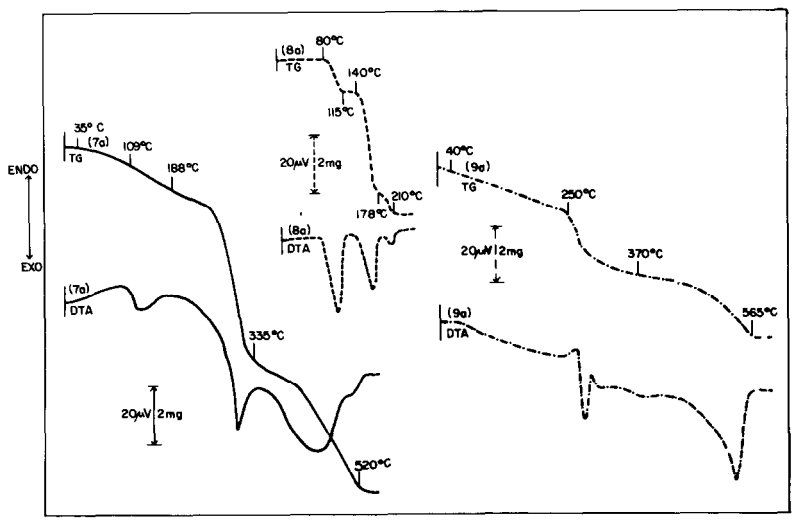

Fig. 3. Thermal curves of $[Cd(pipz)_2(MCA)_2] \cdot 2H_2O$ (**7a**) (17.50 mg) (———), $[Cd(mpipz)_2(MCA)_2]$ (**8a**) (12.06 mg) (- - - - -) and $[Cd(dach)_2(MCA)_2]$ (**9a**) (9.00 mg) (· – · – ·).

CONCLUSIONS

In almost all the complexes, the DTA curves show two peaks, indicating that the decomposition of metal monochloroacetates into metal chlorides occurs in two steps [17,18].

As in our earlier observations [1–3], the order of stability of these complexes (with respect to E_a^*) follows the trend pipz > mpipz > dach (Table 3). *N*-Alkylation of the cyclic ligand should increase the stability of the mpipz complexes due to the increased basicity of mpipz. However, the steric effect causes decreased stability [19,20]. Furthermore, the dach complexes are the least stable (with respect to E_a^*), although the strain in the cyclic ligand can be reduced by introducing a methylene group between the amine functions.

The linear correlation between E_a^* and ΔS (as observed previously [1–3]) indicates that a system with a higher entropy change ΔS will require less energy E_a^* for its thermal decomposition [1–3,11] (Fig. 4).

As mentioned earlier, the values of $\Delta\nu$ (Table 2) are higher than those of acetato complexes [3]. This phenomenon may be due to the electron-withdrawing effect of chlorine on CO_2^- in MCA.

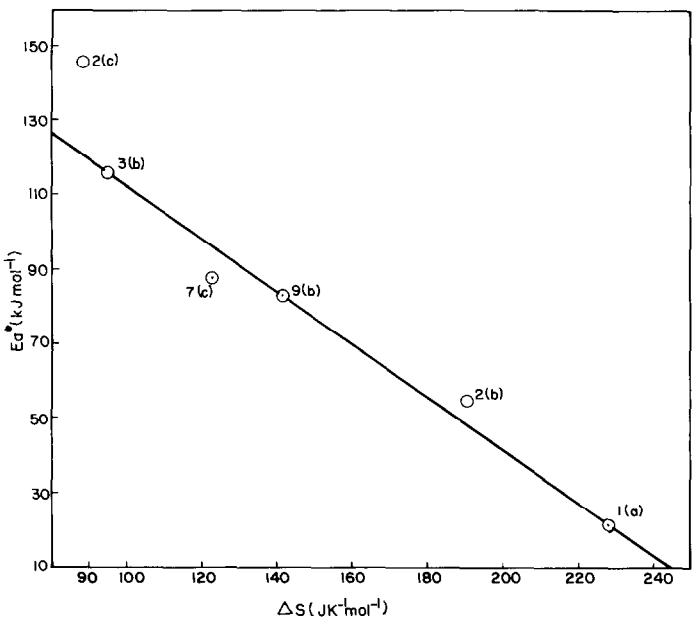

Fig. 4. Plots of E_a^* vs. ΔS for conversions: $[Ni(pipz)(MCA)_2(H_2O)_2] \rightarrow [Ni(pipz)_{0.5}(MCA)_2]$ (1(a)); $[Ni(mpipz)_2(MCA)_2] \rightarrow [Ni(mpipz)(MCA)_2]$ (2(b)); $[Ni(mpipz)(MCA)_2] \rightarrow Ni(MCA)_2$ (2(c)); $[Ni(dach)_2(MCA)_2] \rightarrow Ni(MCA)_2$ (3(b)); $[Cd(pipz)_2(MCA)_2] \rightarrow Cd(MCA)_2$ (7(c)); $[Cd(dach)(MCA)_2] \rightarrow Cd(MCA)_2$ (9(b)).

ACKNOWLEDGEMENTS

The authors are very grateful to the Government of Manipur, Imphal, Manipur, India for granting one of them (L.K. Singh) study leave under FIP of the UGC scheme. They wish to express their thanks to Professor N. Ray Chaudhuri, Department of Inorganic Chemistry, Indian Association for the Cultivation of Science, Calcutta 32, India for his valuable help and encouragement and to CDRI, Lucknow, India for elemental analyses.

REFERENCES

1 L.K. Singh and S. Mitra, J. Chem. Soc., Dalton Trans., (1987) 2089.
2 L.K. Singh and S. Mitra, Inorg. Chim. Acta, 133 (1987) 141.
3 L.K. Singh and S. Mitra, Thermochim. Acta, 138 (1989) 285.
4 P.J. Hendra and D.B. Powell, J. Chem. Soc., (1960) 5105.
5 K. Nakamoto, Infrared and Raman Spectra of Inorganic and Coordination Compounds, 3rd edn., Wiley-Interscience, New York, 1978, pp. 228, 232, 233.
6 A.V.R. Warrier and P.S. Narayanan, Spectrochim. Acta, Part A, 23 (1967) 1061.
7 E. Spinner, J. Chem. Soc., (1964) 4217.
8 A.I. Vogel, A Textbook of Quantitative Inorganic Analysis, 3rd edn., ELBS and Longmans, London, 1968, pp. 389, 390, 480.
9 H.H. Horowitz and G. Metzger, Anal. Chem., 35 (1964) 1464.
10 H.J. Borchardt and F. Daniels, J. Am. Chem. Soc., 79 (1957) 41.
11 R. Roy, M. Chaudhury, S.K. Mandal and K. Nag, J. Chem. Soc., Dalton Trans., (1984) 1681.
12 A.W. Coats and J.P. Redfern, Nature (London), 201 (1964) 68.
13 N.F. Curtis, J. Chem. Soc. A, (1968) 1579.
14 F.A. Cotton and G. Wilkinson, Advanced Inorganic Chemistry, 3rd edn., Wiley-Interscience, New York, 1972, pp. 504, 505.
15 D.F. Steele and T.A. Stephenson, J. Chem. Soc., Dalton Trans., (1972) 2161.
16 S.D. Robinson and M.F. Uttley, J. Chem. Soc., Dalton Trans., (1973) 1912.
17 R.C. Mehrotra and R. Bohra, Metal Carboxylates, 1st edn., Academic Press, London, 1983, p. 123.
18 N. Ray Chaudhuri, S. Mitra and G.K. Pathak, J. Therm. Anal., 16 (1979) 13.
19 W.K. Musker and M.S. Hussain, Inorg. Chem., 5 (1966) 1416.
20 J.E. Huheey, Inorganic Chemistry, 3rd edn., Harper International, New York, 1983, pp. 298, 299.